JOURNAL OF MATERIALS SCIENCE 21 (1986) 1897–1913

The structure of thermotropic copolyesters

LINDA C. SAWYER, MICHAEL JAFFE
Celanese Research Company, 86 Morris Avenue, Summit, New Jersey, USA

Highly oriented polymeric products have been produced over the past fifteen years by two very different processing routes; from conventional polymers processed to highly oriented extended chain structures, and from "rod-like" polymers which exhibit liquid crystalline behaviour. Gel spun polyethylene is an example of such a conventional polymer. There are three main types of liquid crystalline polymers (LCP) which have high orientation and modulus: lyotropic aramids, such as poly(*p*-phenylene terephthalamide) (PPTA); lyotropic, aromatic heterocyclic polymers, or "ordered polymers"; and the family of thermotropic aromatic copolyesters. Extensive characterization of the thermotropic copolyesters has resulted in the delineation of a fibrillar, hierarchial structural model which accounts for the structures observed in a broad range of oriented fibres, extrudates and moulded articles. Three distinct fibrillar species are observed: microfibrils that are about 50 nm, fibrils about 500 nm, and macrofibrils about 5 μm, in size. Superimposed on the structural hierarchy is a defect hierarchy, defined by the regular meander of the molecular chain and a localization of defects within a microfibril at about a 50 nm periodicity. Orientational variations, layering and skin core structures, in thick specimens, are the result of local flow fields on the basic structural units during solidification. The fibrillar textures appear to be present prior to any preparation for microscopy. A wide range of specimen preparation methods, i.e. fractography, sonication, microtomy and etching, and microscopic techniques, i.e. optical, scanning and transmission electron microscopy, were applied to the characterization of the aromatic copolyesters and PPTA. Interestingly, the same basic hierarchy is observed for both the lyotropic and the thermotropic LCPs and the microfibrillar structures of all the highly oriented polymers, including polyethylene, appear quite similar.

1. Introduction

Over the past fifteen years a number of technologies have emerged for producing highly oriented polymeric products with moduli approaching significant fractions of their theoretical values [1–14]. These successful approaches fall into two distinct classes:

1. The careful manipulation of conventional polymers into extended chain structures of near perfect molecular orientation in the solid state.

2. The design of stiff, "rod-like" molecules which exhibit nematic liquid crystalline behaviour in the melt or solution and transform easily into highly oriented, extended chain structures in the solid state.

The "gel spinning" of polyethylene into fibre with a tensile modulus of about 150 GPa [4–6] is perhaps the best example of the first class; other examples include hydrostatic extrusion [7], die drawing [8], and "superdrawing" [9–11]. In addition to polyethylene, high modulus variants of polyacetal [12], polypropylene [13], polyamide-hydrazides [14], and others [2], have been reported.

The liquid crystalline polymers now comprise a vast class with thousands of molecular compositions documented in the literature [1, 15, 16]. Most important among these are:

(a) Poly(*p*-phenylene terephthalamide) (PPTA), the lyotropic aramid commercialized as fibre by the duPont Company under the tradename, Kevlar (e.g. [17]).

(b) "Ordered polymers", a group of lyotropic, aromatic, heterocyclic polymers which exhibit the highest fibre tensile modulus values yet observed [18–20].

(c) Aromatic copolyesters, a large family of thermotropic polymers rigorously investigated in the laboratories of Eastman Kodak [21, 22], duPont [17, 23–25], Celanese [1, 26–33], and others.

Recently, the focus of liquid crystalline polymer research has shifted from the synthesis of new molecules to the understanding of the process–structure–property relationships controlling these novel systems. Experimental observations, models and theories describing chain statistics [34, 35], flow characteristics [30, 31, 36–41], transition behaviour [42], and solid state and mesophase structures [20, 23, 28–32, 40–41, 43–51], now proliferate in the literature. Of special interest are the detailed structural models proposed for the aramid fibres [23, 43, 47, 52], for the ordered polymers [18], and for the non-mesogenic high modulus polyethylene fibres [53–56].

It is the purpose of this paper to add to this emerging database a representative set of morphological observations on the thermotropic copolyesters made in the Celanese laboratories. These results include the structure of fibres and uniaxially oriented extrudates, and shaped extrudates and injection-moulded specimens covering a broad range of average molecular orientations. Observations, ranging from

0022–2461/86 $03.00 + .12

macrostructures to microstructures on the molecular level will be discussed. Results will be organized to isolate general features common to all samples from features peculiar to a specific process history. Finally, a hierarchical model of thermotropic copolyester structural organization will be proposed, unanswered questions highlighted and the whole put into perspective within the framework of the current literature.

2. Experimental details

2.1. Materials

A broad range of thermotropic polymer compositions were studied. Polymers were typically naphthalene moiety containing thermotropic polyesters (NTP) [1], i.e. copolyesters composed of 2,6-naphthyl and 1,4-phenyl units. It was found that, for most of this research, the general NTP nomenclature is adequate. Poly(*p*-phenylene terephthalamide) (PPTA) fibres were also studied, as a control. The term LCP (liquid crystalline polymer) will be used when structures typical of both lyotropic and thermotropic materials are discussed.

2.2. General methods

Traditional methods for the study of polymer morphology include the entire range of microscopical instruments and techniques. Optical microscopy (OM), generally using polarized light (PLM), is useful to observe semi-crystalline materials and to see the effects of orientation, separate phases, and contaminants, as well as providing an overview of structures larger than a micrometre in size. Scanning electron microscopy (SEM) permits a higher magnification view to about 5 to 10 nm resolution of the surface of materials. In the analytical electron microscope (AEM) high resolution secondary electron imaging (SEI) permits direct surface study to 3.5 nm resolution and transmission electron microscopy (TEM) permits the observation of structures to less than 1 nm. This range of instrumental methods requires a variety of sample preparation methods which range from established methods to some developed specifically for liquid crystalline polymers.

2.3. Optical microscopy

A Leitz Orthoplan polarizing optical microscope was used in these studies. Fibres were imaged directly in transmitted light by placing them on a glass slide in an appropriate immersion oil. In the case of thick fibres, strands, rods, and moulded parts, preparation involved sectioning the material thin enough to transmit light. Samples too thick or tough to be successfully microtomed were polished into thin sections (PTS) by methods normally used for ceramics and metallurgical specimens. Composites containing liquid crystalline polymers, and materials such as glass fibres, are also prepared by the PTS method to observe their distribution and orientation in polarized light.

A dynamic, high resolution, programmable hot stage-polarized light microscope system was developed for the evaluation of thermotropic liquid crystalline polymers at elevated temperatures. A colour video camera, or a still 35 mm camera, were used to record the sample appearance, while a photometric recording system provided a trace of light transmittance through the sample as a function of temperature.

2.4. Scanning electron microscopy

Scanning electron microscopy was conducted by standard techniques, as described by Goldstein *et al.* [57]. The Scott [58] method of peel-back was applied to determine the internal structure of fibres. Fibres were prepared by nicking them with a scalpel and peeling them back with fine forceps to reveal internal or bulk textures. The structures typical of fibres, extruded strands or rods, moulded parts, composites and polymer blends were observed by SEM study of fractured specimens. A potential artefact of fractography is that the fracture event may be the origin of the structures observed. The Amray 1000 SEM was used in these studies.

2.5. Analytical electron microscopy

Ultrathin samples are required for the TEM imaging modes while thicker samples (about 1 to 3 mm) can be imaged in the SEI mode. Following the work of Dobb *et al.* [46] a high power ultrasonic device was used to disintegrate or pulp LCP fibres, providing fine "fibrillar" materials thin enough to image in the TEM and for electron diffraction. Diamond knife microtomy was used to provide intact, longitudinal sections between about 50 and 100 nm thick [28]. Sections were examined by bright-field imaging, and by diffraction methods, such as dark-field (imaging), selected-area electron diffraction (SAD), and microdiffraction, in the JEOL 100CX. The spatial resolution of X-ray diffraction is several millimetres in diameter, while that of selected-area electron diffraction is about 1 μm; in micro-diffraction the spatial resolution can be as small as 20 nm. Studies of thermotropic polymers [51, 59] and determination of the separate phase structures coexisting in poly(ethylene terephthalate-co-*p*-hydroxy-benzoate) (X7G®) fibres [28], were determined by this technique. High resolution SEI micrographs are formed from surface secondary electrons with a resolution of about 3.5 nm [60]. SEI techniques have been developed to elucidate polymer fine structures [60, 61].

2.6. Plasma and ion etching

Plasma and ion etching are methods employed to prepare specimens for microscopic observation of bulk or internal structures. Etching methods are known to cause potential artefacts. Plasma etching studies were conducted in a low temperature plasma asher (LTA). This device was shown to provide a non-directional oxygen plasma which minimized artefact formation. Oxygen and argon were used at 162° C, at times of 5 to 30 min. Ion etching was performed with the Ion Tech ion beam micro-sputter gun. Structural results from both etching techniques were similar.

3. Results

3.1. Uniaxially oriented extrudates

Observation of the texture of small molecule liquid

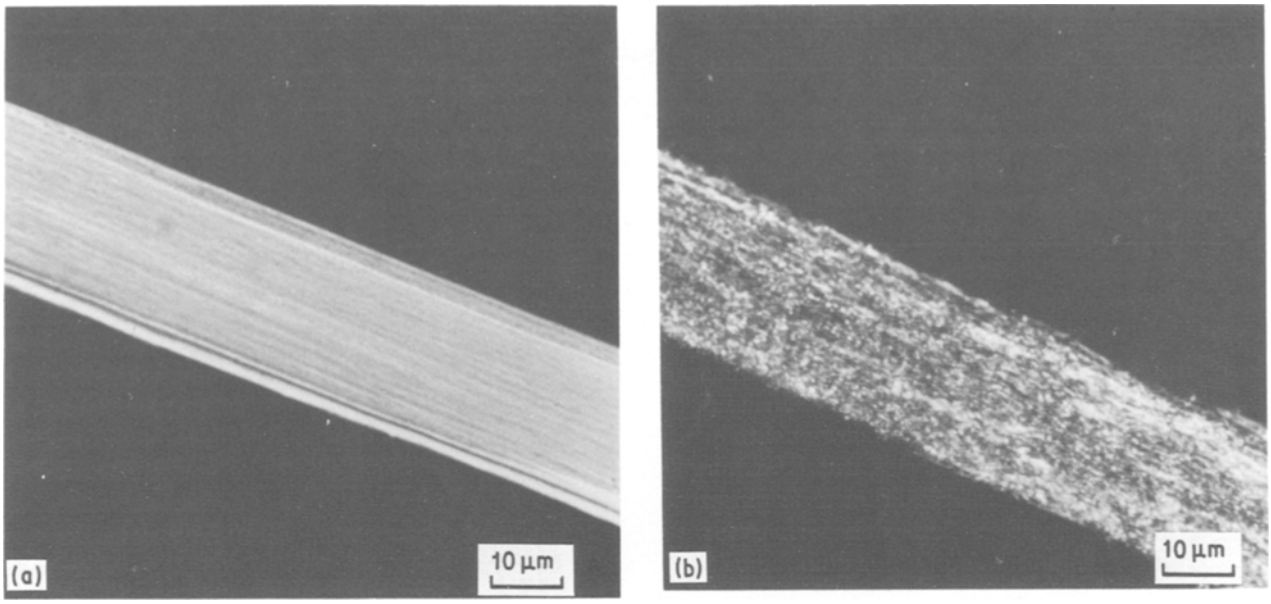

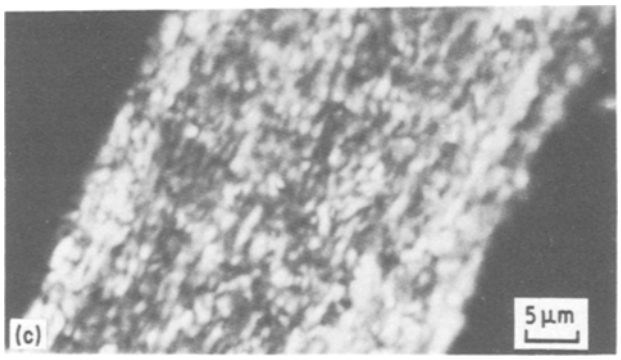

Figure 1 Observation of a thin section of a highly oriented tape, at 45 degrees to the crossed polarizers (a), shows it is highly birefringent. A fine "salt and pepper" texture is seen when the section is in the orthogonal position (b) revealing incomplete extinction of the polymer. A higher magnification view of the area in (b) shows a fine "domain" texture, elongated in the axial orientation direction (c).

crystals, in the optical microscope, reveals typical phase structures [62, 63] which are important in describing these materials. Accordingly, optical investigation of liquid crystalline polymers was undertaken which proved useful in the definition of the structure and for comparison with the small molecule analogues. Optical study of a uniaxially oriented NTP fibre or thin tape, viewed in a polarizing microscope at 45 degrees to the polarization direction (Fig. 1a), shows the polymer is highly oriented with no apparent fine structure, as expected. When these sectioned fibres or tapes are observed in the orthogonal position in polarized light they exhibit a faint "salt and pepper" texture and thus incomplete extinction, as shown in Fig. 1b. This observation of incomplete extinction, also observed for Kevlar [64], is unexpected, as highly oriented fibres generally exhibit complete extinction when oriented parallel to either polarization direction [64]. High magnification (up to $\times 1600$) micrographs (Fig. 1c) reveal textures that may be described as "domain-like", i.e. regions of high local order. The domains observed in oriented structures are about 0.5 μm across (500 nm), elongated along the fibre axis. The colour variation between domains is of the same order, and thus is not the result of major orientational variations. Such colour variations may be the result of small orientation variations within the plane of the section or they may be accounted for by a slight out of plane tilt, or serpentine trajectory, of the molecules within a domain, compared to adjacent domains. This theme will be developed further in the discussion of extrudates, as a periodic 500 nm structure, observed as striations perpendicular to the fibre axis, is termed a lateral "banded texture" in less well oriented NTPs. This interpretation is consistent with studies of NTP sheared films by Donald and Windle [50] who have suggested that banding, also on a scale of about 500 nm, is associated with a "serpentine" path of the molecules about the shear direction. Additionally, this interpretation is somewhat analogous to the "meander" reported for poly(*p*-phenylene benzobisthiazole) (PBT) [18], and the "pleated sheet" structures reported in some PPTA fibres [43]. The variation observed in the NTPs is more a meander, or serpentine, than the sharp pleat observed in PPTA. The reported periodicity is about 500 nm [16, 43, 65] in PPTA and also about 500 nm in the NTPs reported here.

Highly oriented NTP extrudates (fibres, tapes, etc.) show a longitudinally oriented "fibrillar" microstructure when prepared and observed by various microscopical techniques. By "fibrillar" is meant structures of high aspect ratio, although these are not necessarily structures exhibiting strict fibre symmetry. In most cases, "tape-like" is a more accurate description and often the structures appear to be uniaxially oriented sheets. Fibrillar structures are observed by optical microscopy of specimens peeled apart or fractured and often fine fibrils are seen of the order of 500 nm wide, elongated with the fibre axis. Fibrillar, tape-like structures have also been observed in the SEM of fractured fibres of both NTPs (Fig. 2a to d) and for Kevlar (Fig. 3). Unless otherwise stated discussions of fibril sizes refer to the smallest dimension noted. Fractography of typical NTP fibres reveals a distinct surface skin and a regular fibrillar internal structure

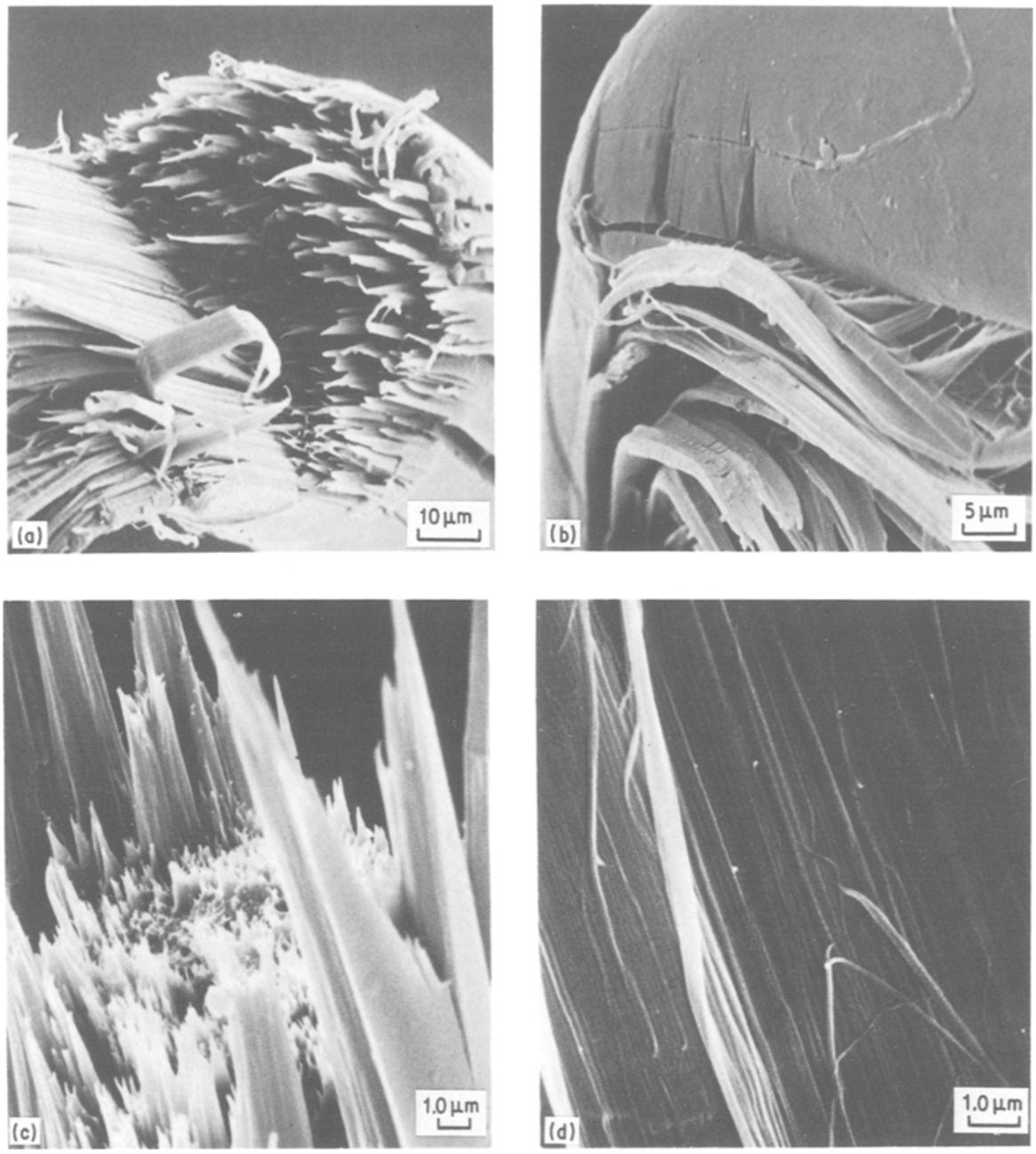

Figure 2 Fractured, uniaxially oriented fibres exhibit a fibrillar microstructure when examined in the SEM. Tape-like structures (a), fibrillar fracture and a coherent surface skin (b and c), and fine fibrils (d), are all typical of NTP fibres.

with a characteristic size of about 5 μm, as illustrated in Fig. 2. It is generally observed that the strength of the fibre correlates with fibrillarity of the fracture surface and the length of the fibril "pull outs". Similar results have been published for PPTA fibres [23] and an example of a fractured Kevlar fibre is shown in the scanning electron micrograph in Fig. 3.

Fibrils observed in the TEM following sonication are shown in Fig. 4. This method permits evaluation of the finest microstructures present in these materials. Fig. 4a shows a fibril of PPTA; its selected-area diffraction pattern shows the oriented nature of the structure. A fibril from a sonicated as-spun NTP, shown in Fig. 4b, exhibits a fine texture perpendicular to the fibre axis which will be termed a "microbanded" texture. The periodicity of the observed microbanding, about 100 nm, and the size of the bands (50 nm or 0.05 μm), are interestingly an order of magnitude smaller than the banded textures observed in extrudates (below) and in sheared films [49, 51], and this may suggest a relationship to the serpentine molecular trajectory model described above. Shadowing, used to highlight the three dimensionality of fibrils (Fig. 4d), reveals that these fibrils range in size down to 50 nm and that they are thinner than they are wide.

A fibril from an annealed NTP (Fig. 4c) did not exhibit the microbanding observed in the as-spun fibre. Although the diffraction pattern in the as-spun fibril is weak and too short-lived to record, the pattern for the annealed fibril was sufficiently stable to allow an SAD pattern to be recorded (inset in Fig. 4c). Annealing appears to cause a general perfecting of the fibrillar fine structure of the fibre. The outer skin surface, present in all LCP forms, becomes more coherent after annealing. This increased perfection is also seen within the fibres, as shown in transmission

Figure 3 A fractured Kevlar fibre is seen to be highly fibrillar when viewed in this scanning electron micrograph.

electron micrographs of ultrathin sections (Fig. 5). Internal textures appear more fibrous as-spun (Fig. 5a), and more sheet-like after annealing (Fig. 5b). Selected-area electron diffraction studies of both fibrils and sectioned fibres show sharper, longer lasting diffraction patterns after annealing. This has also been shown by X-ray diffraction studies of aromatic copolyesters [66] and is consistent with both X-ray and electron diffraction studies of PBT [67]. The transmission electron micrographs show that the sectioning process itself reflects a more "rubbery" texture in the as-spun fibres. The data all suggest an increase in lateral order and overall perfection of the structure occurs upon annealing.

Plasma-etching studies were conducted on flat, oriented NTP ribbons. The controls for these experiments are shown in the SEI micrographs in Fig. 6. As expected, neither glass fibres (Fig. 6a) nor amorphous PET film (Fig. 6b) show regular structures after etching. Oriented materials, such as PPTA and PET fibres, shown in scanning electron micrographs in Figs 6c and d, respectively, do exhibit striations perpendicular

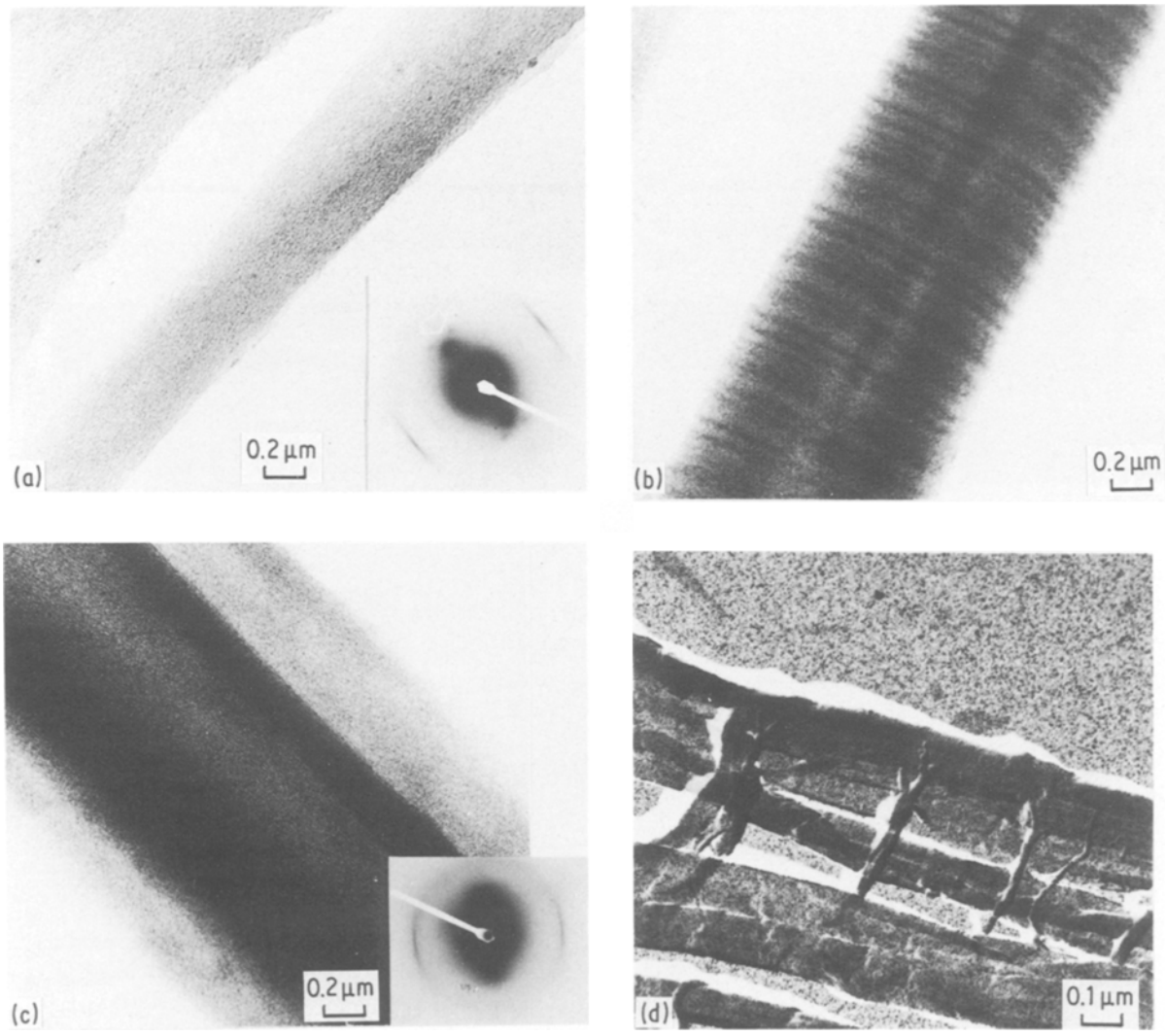

Figure 4 Fibrils are shown in transmission electron micrographs of sonicated fibres. PPTA fibrils (a) exhibit fibre orientation, as shown in a SAD pattern (inset in a). A fibril from an as-spun NTP(b) shows a microbanded texture, whereas no microbanding is observed in an annealed NTP (c). Selected-area electron diffraction could only be recorded for the annealed NTP (inset, c). Shadowing (d) is used to highlight the three dimensionality of the fibrils.

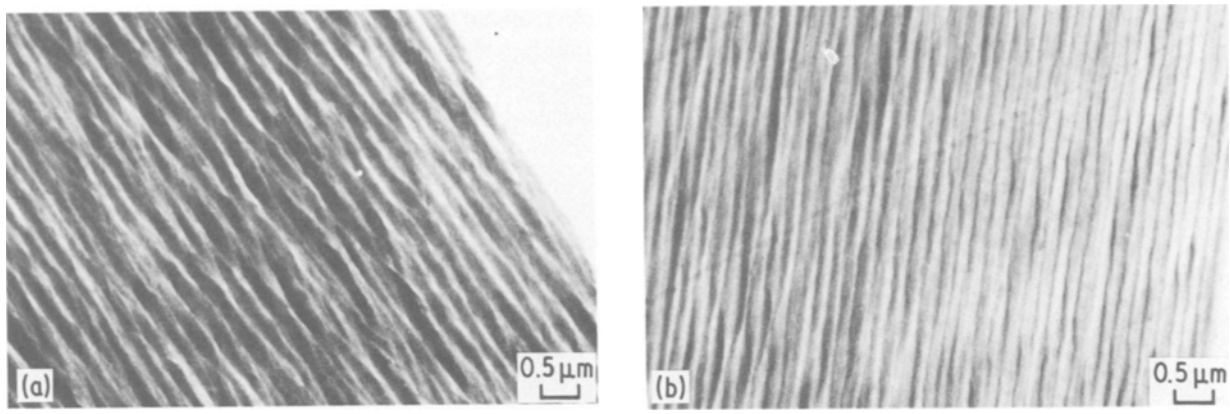

Figure 5 Ultrathin longitudinal sections of as-spun (a) and annealed (b) NTP fibres show axially fibrillar order, with a finer and more coherent structure after annealing.

to the fibre axis. A scanning electron micrograph of an NTP ribbon surface, before etching, is shown to have a coherent surface skin (Fig. 7a). Etched NTP ribbons are shown in Figs 7b and c by SEM, and in the SEI micrograph in Fig. 7d. Submicrometre striations, normal to the draw direction, are observed with a periodicity of about 50 nm. This type of lateral structure has been observed earlier for oriented fibres [68, 69], and a periodic structure of about 35 nm has been reported for Kevlar [23, 52, 70], which has been attributed to the existence of defect layers in the fibre structure [52].

Fibres, films, ribbons and other NTP structures, extruded at relatively high drawdowns from the melt, all have in common the well oriented, fibrillar (sheet-

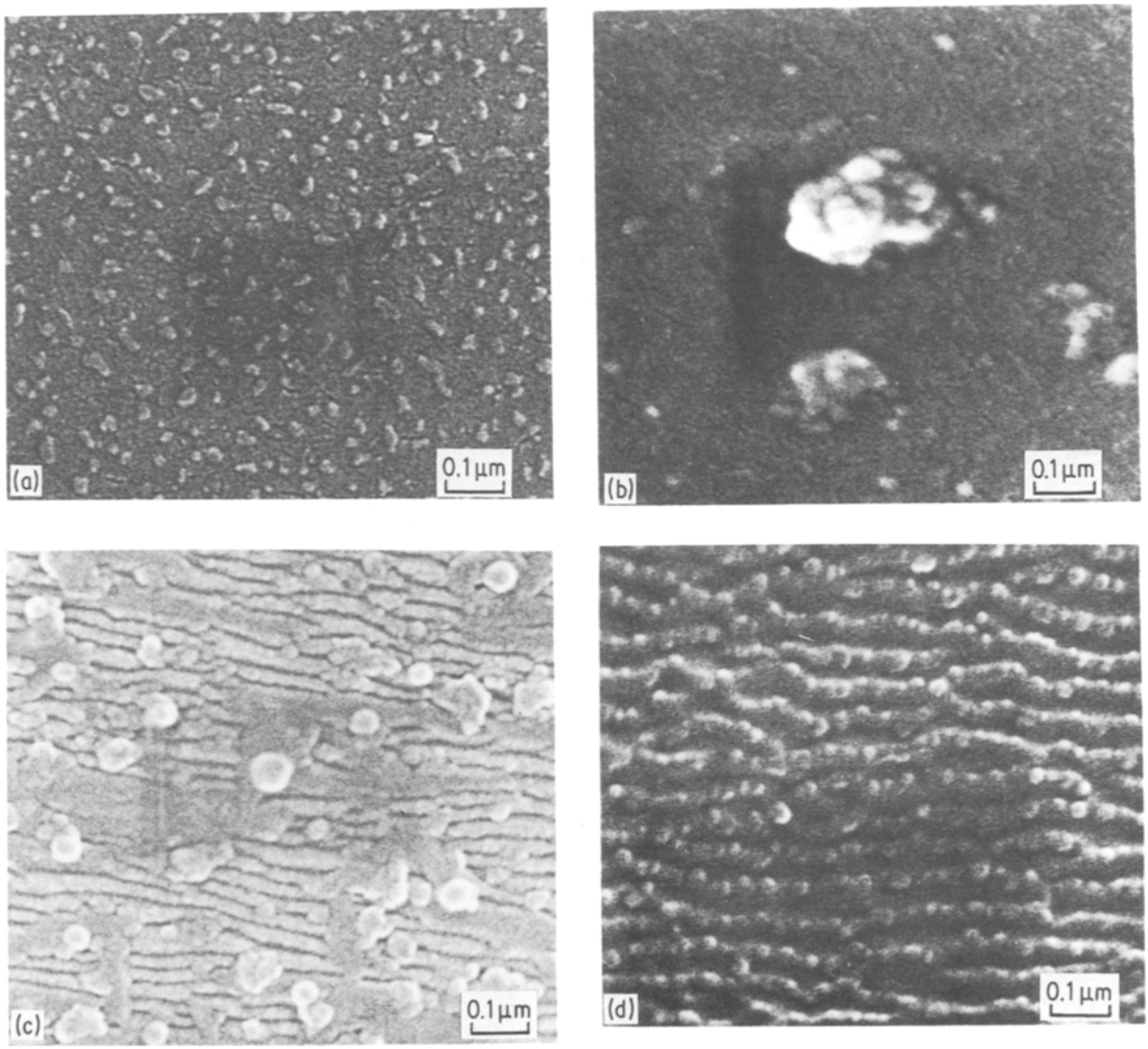

Figure 6 SEI micrographs of fibres following plasma etching with argon reveals a range of textures. Etched glass fibres (a) have fine surface protrusions but no ordered structure and an amorphous poly(ethylene terephthalate) (PET) film surface shows evidence of internal particles. Both PPTA (c) and PET (d) fibres exhibit lateral striations, normal to the drawn fibre axis.

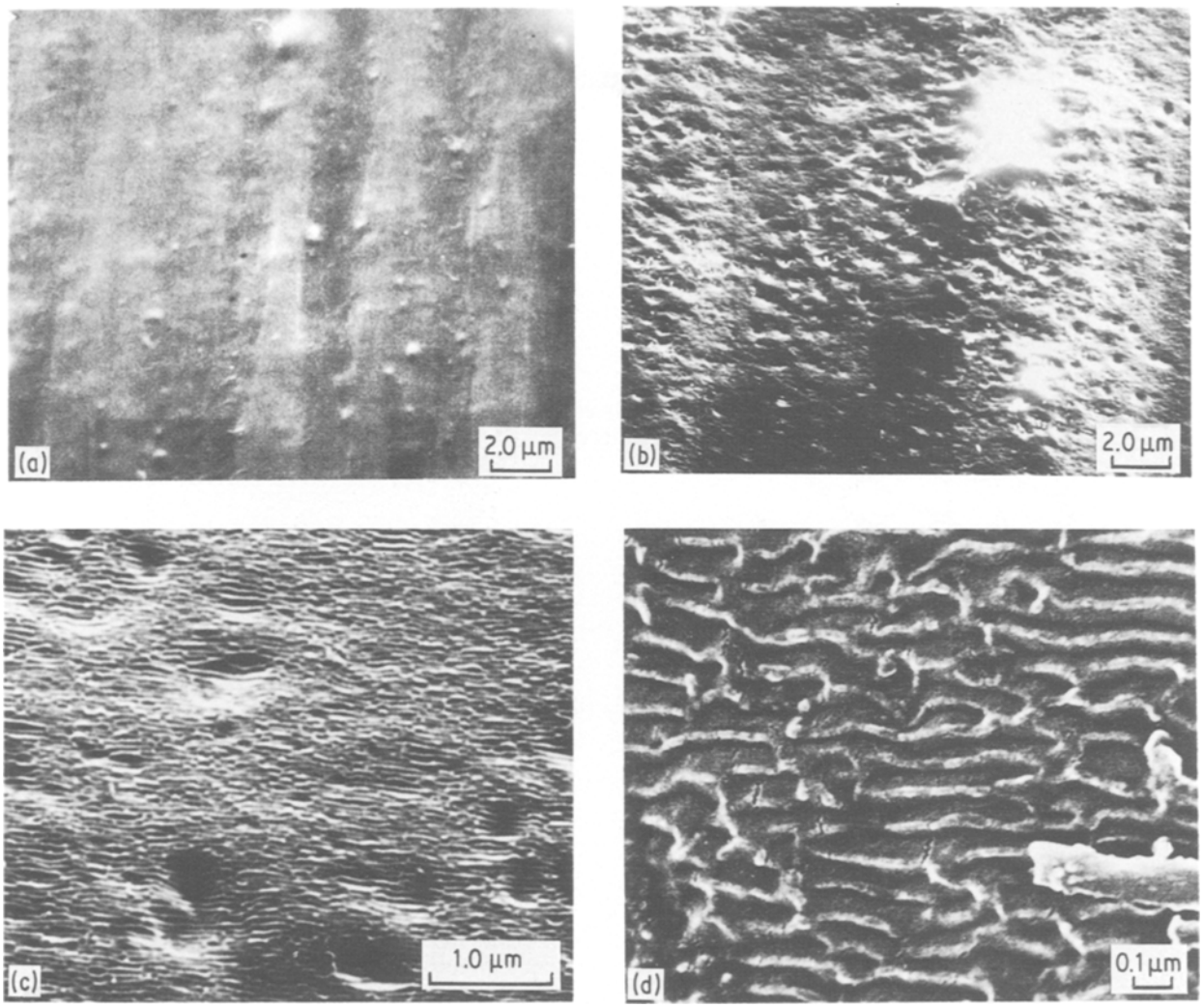

Figure 7 The surface of an untreated, oriented ribbon, prior to etching, is shown in the scanning electron micrograph (a) to have a coherent skin and an axial (vertical) fibrillar texture. Following plasma etching a laterally oriented pattern is observed in the scanning electron micrographs (b and c) which is more clearly shown in the SEI micrograph (d).

like) texture generally associated with highly oriented, extended chain, high modulus polymer extrudates. The size of these structures is of interest because of their hierarchical nature, which appears similar in nature to the structural "hierarchies" first observed for PPTA by Dobb *et al.* [46]. The structural model observed for all LCP oriented structures is shown in Fig. 8. Tape-like macrofibrils, about 5 μm in diameter, are observed in peeled fibres (SEM, top two micrographs in Fig. 8), fracture surfaces (SEM, Figs 2 and 3), and in ultrathin sections (TEM, third figure down in Fig. 8). Fibrils, of the order of 0.5 μm (500 nm) wide, are observed in fracture surfaces (SEM, Fig. 2), peeled fibres (SEM, top two micrographs in Fig. 8), etched ribbons (SEM, Fig. 7), and in ultrathin sections (TEM, third figure down in Fig. 8). The fibrillar dimension is the same as the domain width (OM, Fig. 1), consistent with the observation that when fibrils are pulled or fractured apart in the optical microscope they are seen to be one domain in width (500 nm) and very long. In PPTA the analogous fibrils are also about 500 nm with periodic lateral banding observed at this same dimension. Microfibrils appear, on average, to be about 0.05 μm (50 nm); these are seen in ultrathin sections (TEM, third figure down in Fig. 8), sonicated fibres (TEM, last figure in Fig. 8) and in etched materials (Fig. 7). In PPTA the analogous microfibrils appear to be about 0.03 μm (30 to 40 nm) in size. The finest structures observed in the NTP fibres are of the order of about 5 nm in thickness and in PPTA these structures are about 3 nm in size.

In summary, the NTP oriented extrudate structural hierarchy is composed of: macrofibrils, about 5 μm diameter; fibrils, about 0.5 μm (500 nm) across and, microfibrils, that are about 0.05 μm (50 nm) wide and 5 nm thick. This hierarchy is illustrated in the LCP fibre structural model, shown in Fig. 8. The serpentine trajectory of the molecules (regular in and out of plane tilting) and the etching results suggest that in addition to the structural hierarchy there may be a "defect hierarchy" inherent in LCP structure. The term "defect hierarchy" is used to describe any periodic deviations from a rod-like behaviour or packing observed along the molecular axis.

3.2. Thick extrudates and moulded parts

The microstructure of thick extrudates (lateral dimensions all much greater than fibre dimensions) and moulded bars are composed of the hierarchial units equivalent to those described for LCP fibres, with the

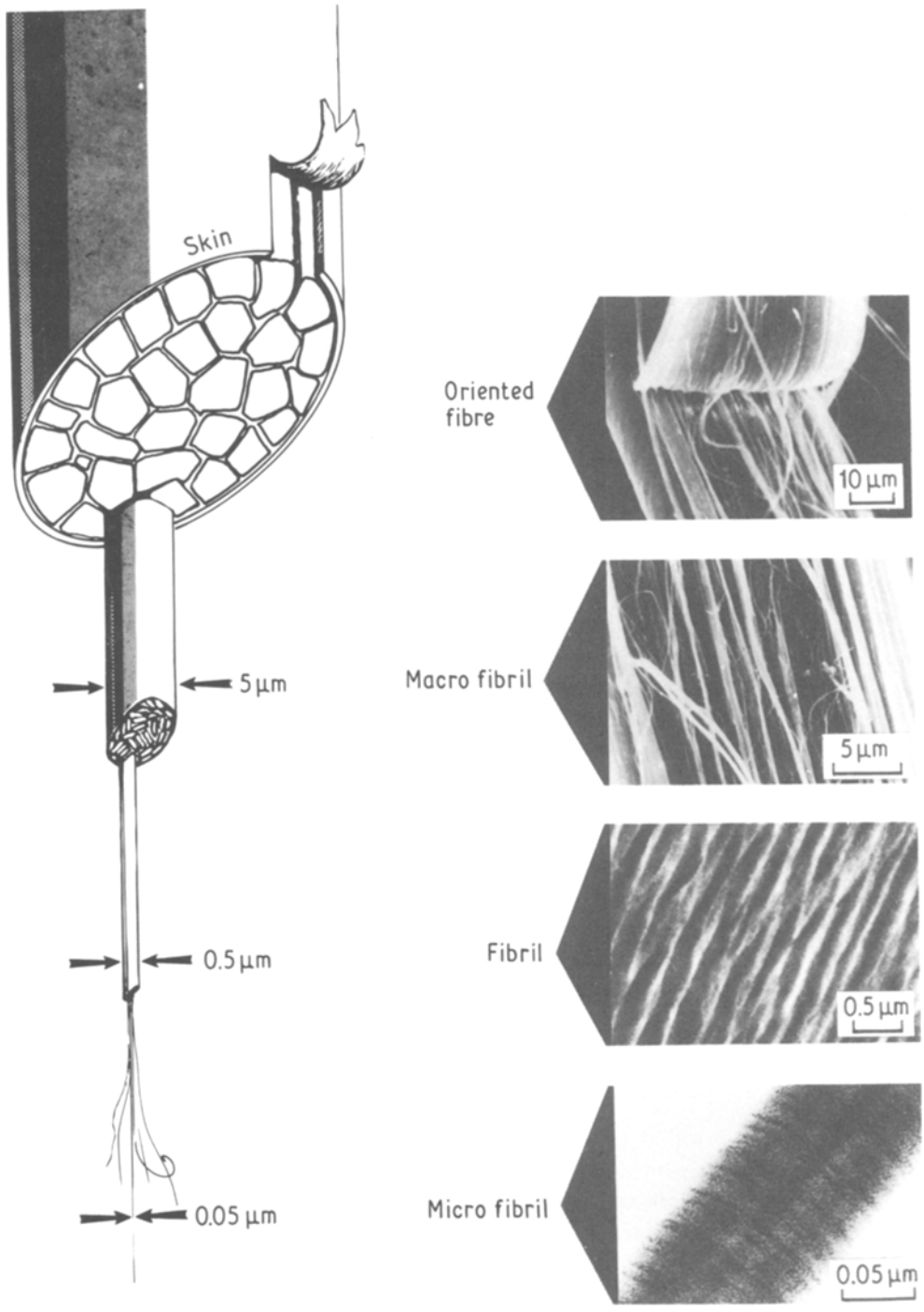

Figure 8 The LCP structural model shows the hierarchial, fibrillar texture of LCP materials in an artist's drawing (left) and in micrographs of oriented materials (right).

added complications of structural macrolayers, major skin core effects and orientational variations. Finite diameter strands exhibit a highly oriented outer skin (as in fibres), axially oriented inner skin layers and, generally, a randomly oriented core. Similar structural features are noted in moulded parts, with complex yet regular variations of molecular orientation superimposed. The skin core texture has been commonly observed in both extrudates and moulded parts, as documented in the literature for LCPs [30, 31, 41, 71] and for typical thermoplastics [72, 73].

Polished thin sections of extruded rods, viewed in polarized light (Fig. 9), clearly show the oriented skin (top of the micrographs) and the less well-oriented core of the rod. A fine domain texture, observed in the core, and to a lesser extent in the skin, is the major optical texture present. Incomplete orientation in the skin causes these domains to be elongated and yet irregular, whereas they are more rounded in the unoriented core. Flow lines [30, 31] are observed in the core, remarkably similar to the bands observed in sheared films of other polymers [49, 50]. The bands observed optically in sheared films are due to periodic variations in orientation of the principal optical vibration directions about the shear axis while the bands in the solid extrudates appear similar and aligned about the fibre axis. The origin of these lateral structures might well be the serpentine molecular trajectory described above. The ratio of skin to core increases with increasing drawdown ratio (increased molecular

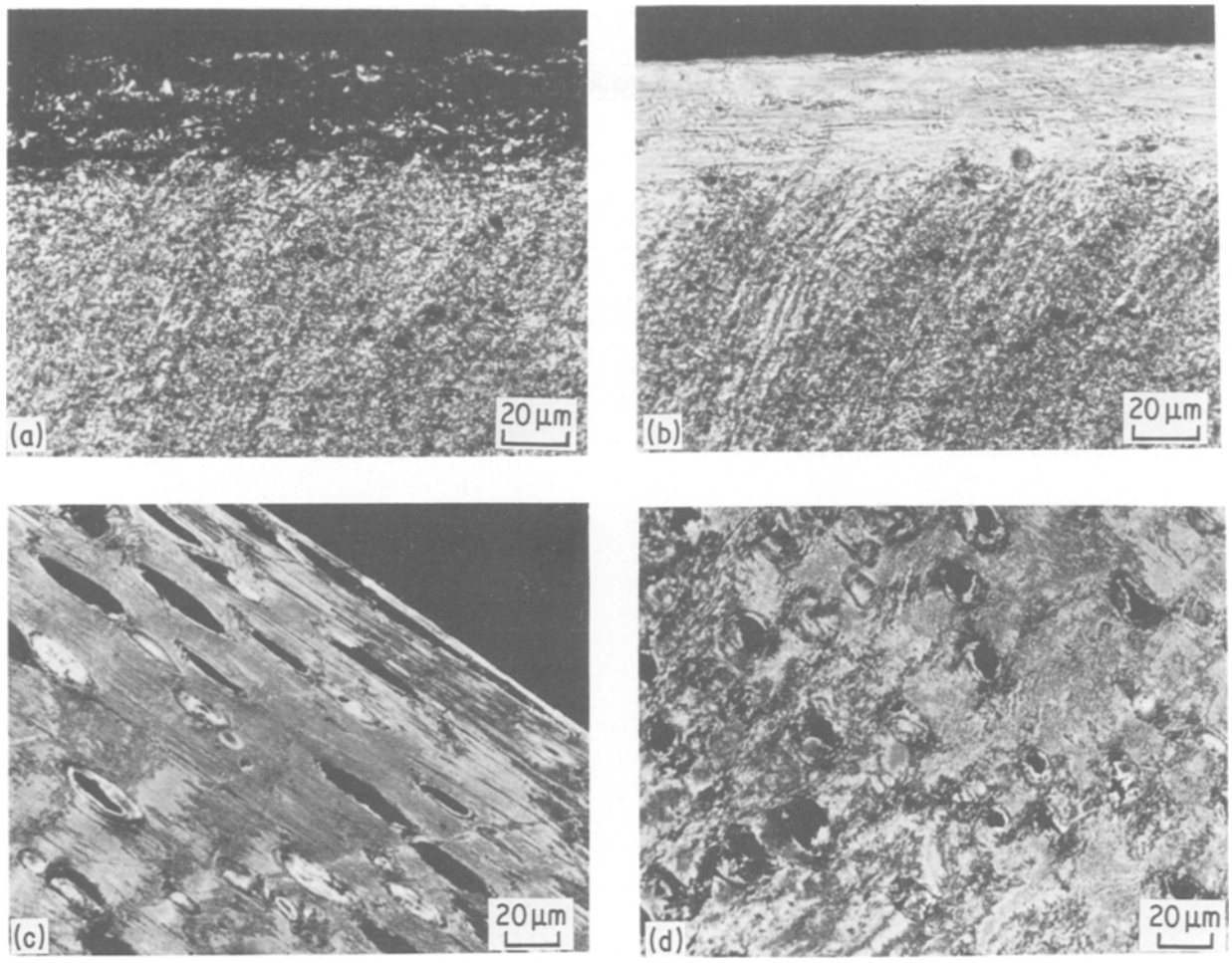

Figure 9 Polarized light micrographs of an extruded rod thin section reveal a partially oriented skin and an unoriented core. Comparison of the section shown in the orthogonal position (a) and at 45 degrees to the crossed polars (b) shows the orientaton of the skin (top) compared to the core. A section of a rod containing voids clearly shows this skin (c) orientation compared to the core (d) as the voids are elongated in the former and rounded in the latter.

orientation), and the boundaries between skin and core are sharp and distinct.

A domain texture similar to that seen in the core of thick rods has also been observed in NTP melts utilizing the thermo-optical system described above. The domain textures are similar whether the melts are derived from thin slices of the extruded rods or polymer powders. Domain textures are shown in Fig. 10 where the structure in a section cut from a solid state specimen (a) is compared to the structure observed at elevated temperature (b). This domain texture can be described as a schliern or nematic texture, and is equivalent to the textures seen with small molecule, nematic liquid crystals [62, 63]. This texture is more difficult to isolate in thin sections of solid polymers at room temperature, because of overlapping structure effects in these thicker materials, although highly magnified micrographs (Fig. 10a) show the texture more clearly.

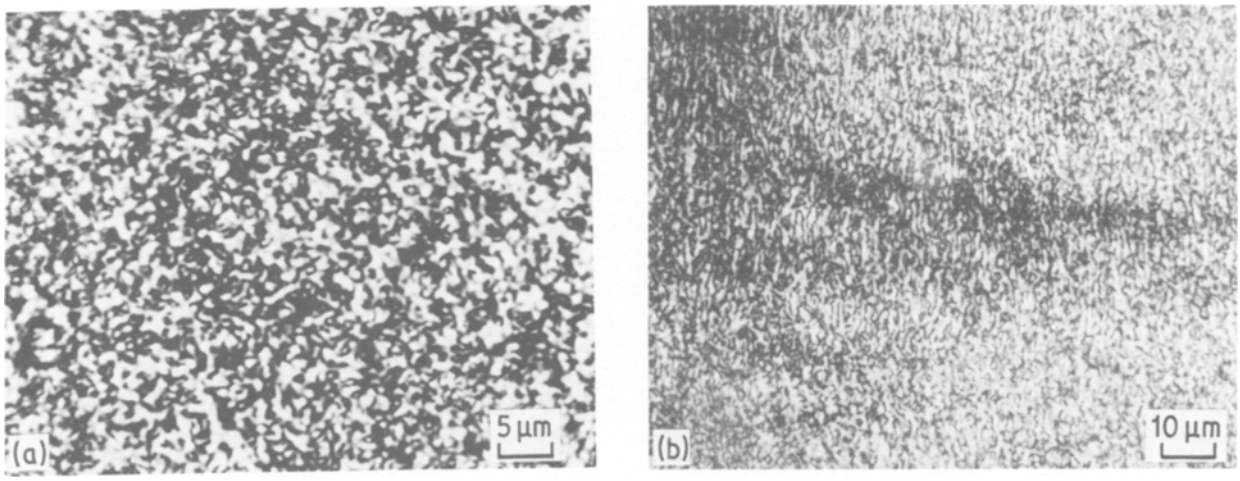

Figure 10 Polarized light micrographs show a detailed view of the nematic domain texture in a section cut from a solid state specimen (a) and a similar texture observed at elevated temperature (b).

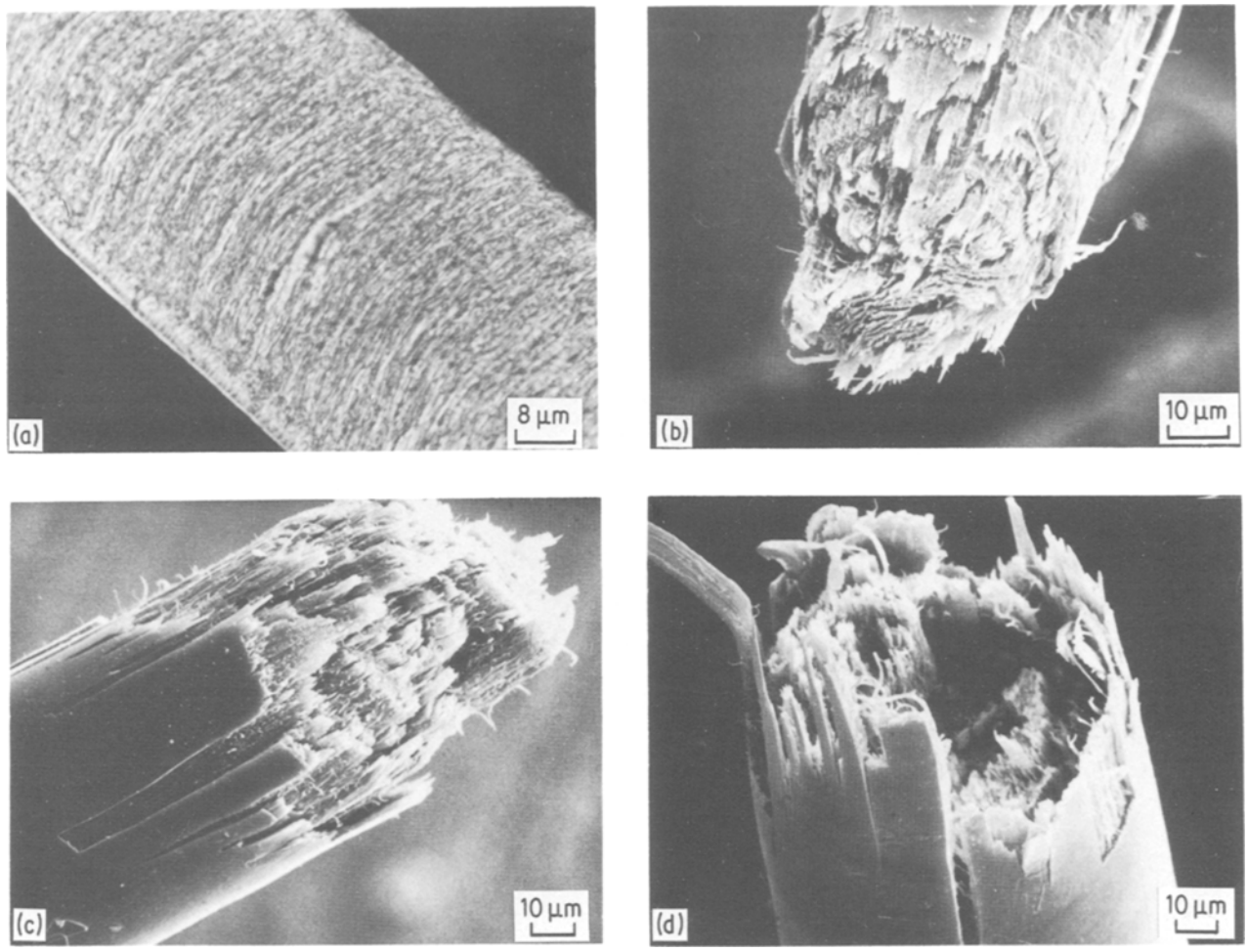

Figure 11 Structures arranged perpendicular to the axis and a surface oriented skin are observed in a polarized light micrograph of a free-fall strand (a). Fractured strands, shown in scanning electron micrographs (b to d) exhibit a sheet-like, fibrillar texture and a coherent surface skin.

Low average orientation rods, produced by allowing the polymer to "free fall" from a jet, also exhibit lateral structures and a surface, oriented skin, as shown by polarized light microscopy of a longitudinal polished thin section (see Fig. 11a). The smooth surface skin and sheet-like texture of the core of these fractured samples is clearly indicated in the scanning electron micrographs in Figs. 11b to d. As orientation is increased, the ratio of skin to core increases (Fig. 12a) and longer, more fibrillar structures are observed, as shown in the micrographs in Figs 12b to d. Fine, submicrometre, sheet-like fibrils are observed in the fracture surfaces (see Figs. 11b to d and 12b and c). The variations in the layered structures and the skin core phenomena observed can be correlated to the process history and the polymer details [30, 31]. Using a composite mechanics approach [74, 75], the relationship between the structure and physical properties is being established.

NTP moulded bars exhibit a layered structure, with macrolayers of sufficient thickness to be visible to the naked eye, as shown in Fig. 13. Fig. 13a is a low magnification reflected light micrograph of a polished moulding and Fig. 13b is a more detailed view, of another bar, where lateral layers or flow lines, and structures arranged longitudinally are both visible, illustrating the importance of the detailed process history in determining the structure of LCP mouldings [41]. Microtomy of moulded bars is difficult but sections exhibit a domain structure (Fig. 13c). The domain texture is indistinct due to the thickness of the sections. Fracture surfaces of moulded bars, observed in the scanning electron micrographs, in Fig. 14, reveal these layers in more detail. Fig. 14a shows the coherent surface skin, while a layered texture is shown in the fracture surface in Figs 14b and c.

The microstructure of moulded bars can be described according to the local orientation imposed by the process. Beginning with the uniaxial outer skin, oriented parallel to the mould filling direction, a series of layers are observed which differ in average orientation with respect to one another, as well as in the perfection of orientation within any given layer. In general, perfection decreases as one proceeds from skin to core. As the resolution of the viewing technique is increased, macrolayers are found to consist of thinner layers which are themselves composed of microlayers. The one exception to this is the central core which has little or no orientation and is relatively featureless. Similar results have recently been published by Weng *et al.* [71], showing the texture of mouldings by SEM study.

To further elucidate internal microstructure, etching experiments and X-ray diffraction were performed on thick extrudates and moulded parts. Polished rod sections exhibit flow patterns and layered structures when viewed in reflected light, as shown in Fig. 15a.

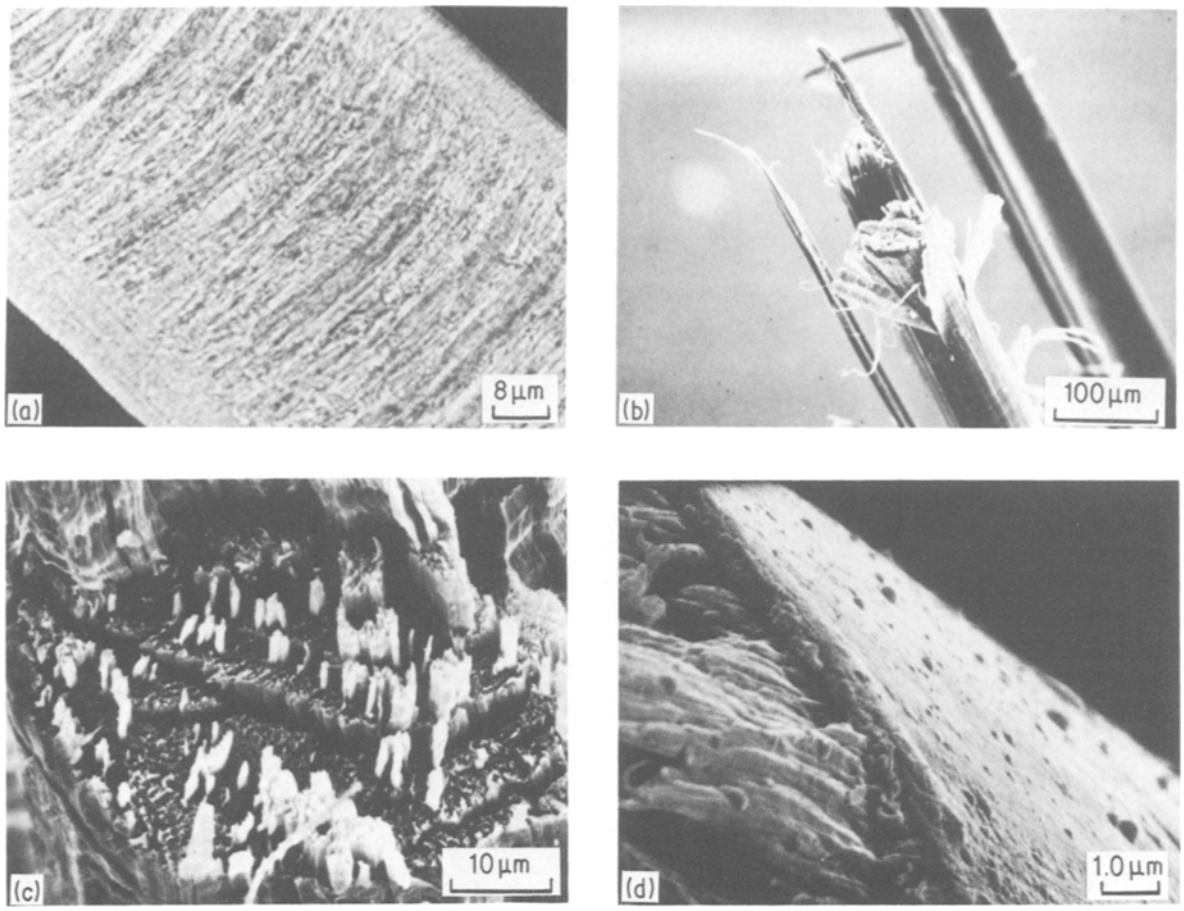

Figure 12 A more highly oriented strand, shown in a polarized light micrograph (a), is seen to have a higher skin/core ratio than the free fall strand in Fig. 11. Fractured strands, shown in the scanning electron micrographs (b and c), have a more pronounced fibrillar fracture (b). Detailed examination shows a coherent skin which differs from the fibrillar core (d).

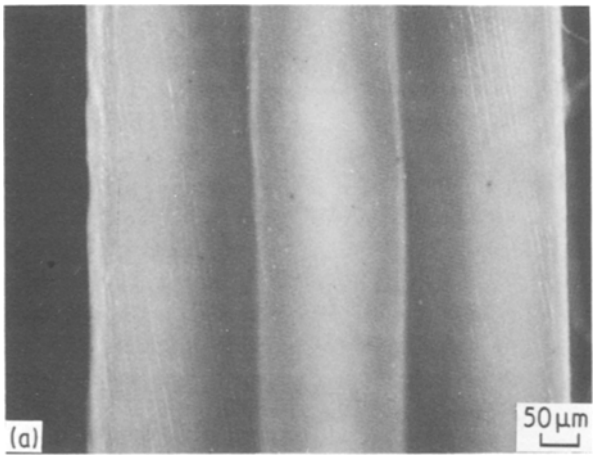

The fine domain texture observed in transmitted polarized light (Fig. 15b) indicates some orientation is present in the skin. SEM studies of these polished surfaces revealed little about the underlying fine structure (Figs 15c and d) until the surfaces were plasma etched. The flow direction of the extruded rod is aligned vertically in the SEI micrographs of the argon-etched strand, shown in Fig. 16. The overview (Fig. 16a) shows an area about one-third of the way into the rod with a "grain", or domain, texture uncovered by the

Figure 13 Reflected light microscopy of polished moulded bars shows a layered structure (a) and structures frozen in due to parabolic-shaped flow lines in the polymer (b). Polarized light micrographs show a fine domain texture (c) is present.

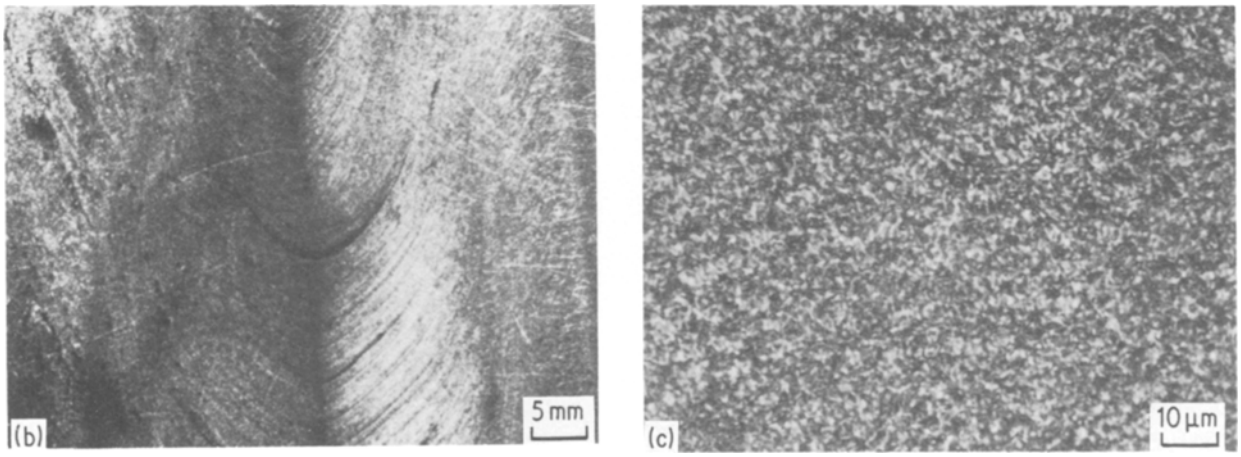

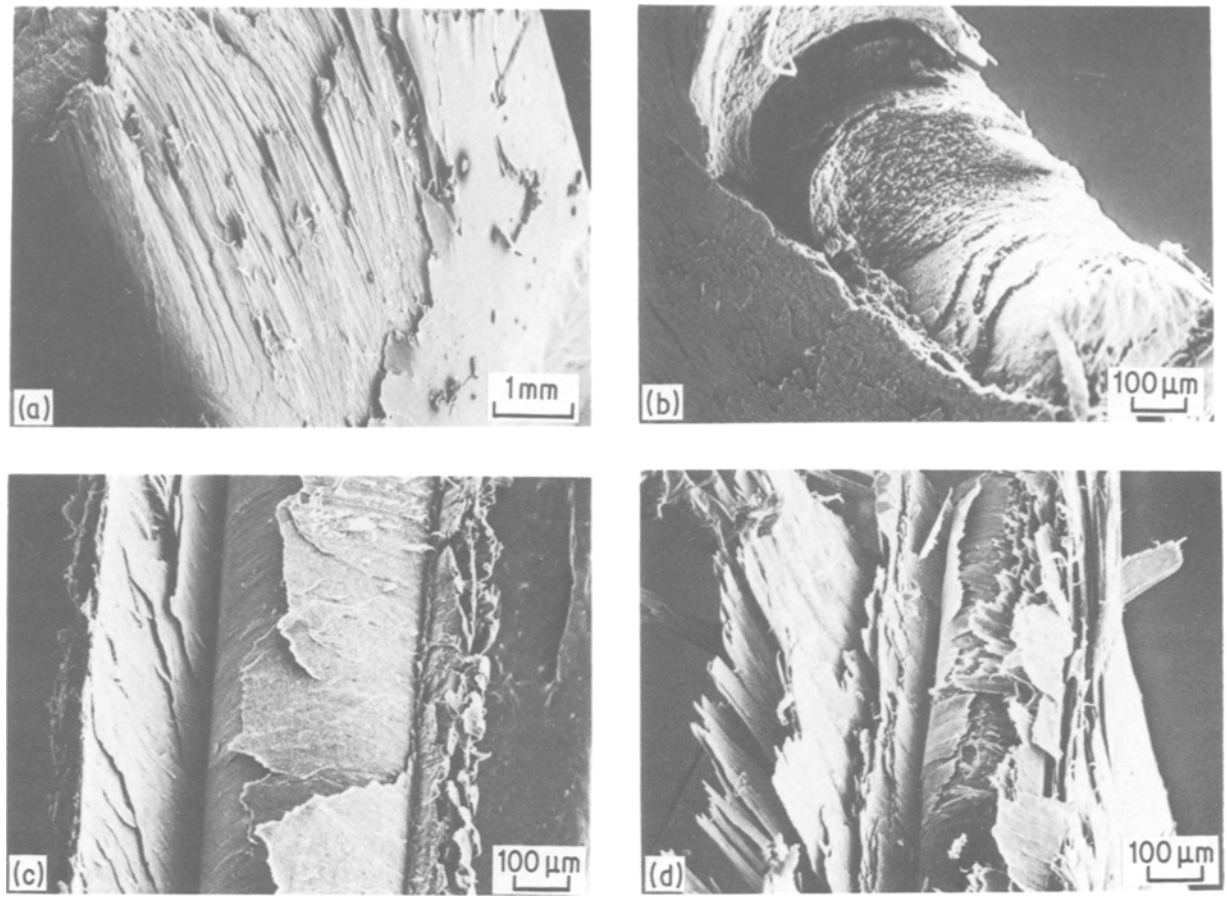

Figure 14 Fractured moulded bars, examined in the SEM, reveal a fine coherent surface skin (a) and lateral layers (b and c) superimposed on a skin core texture.

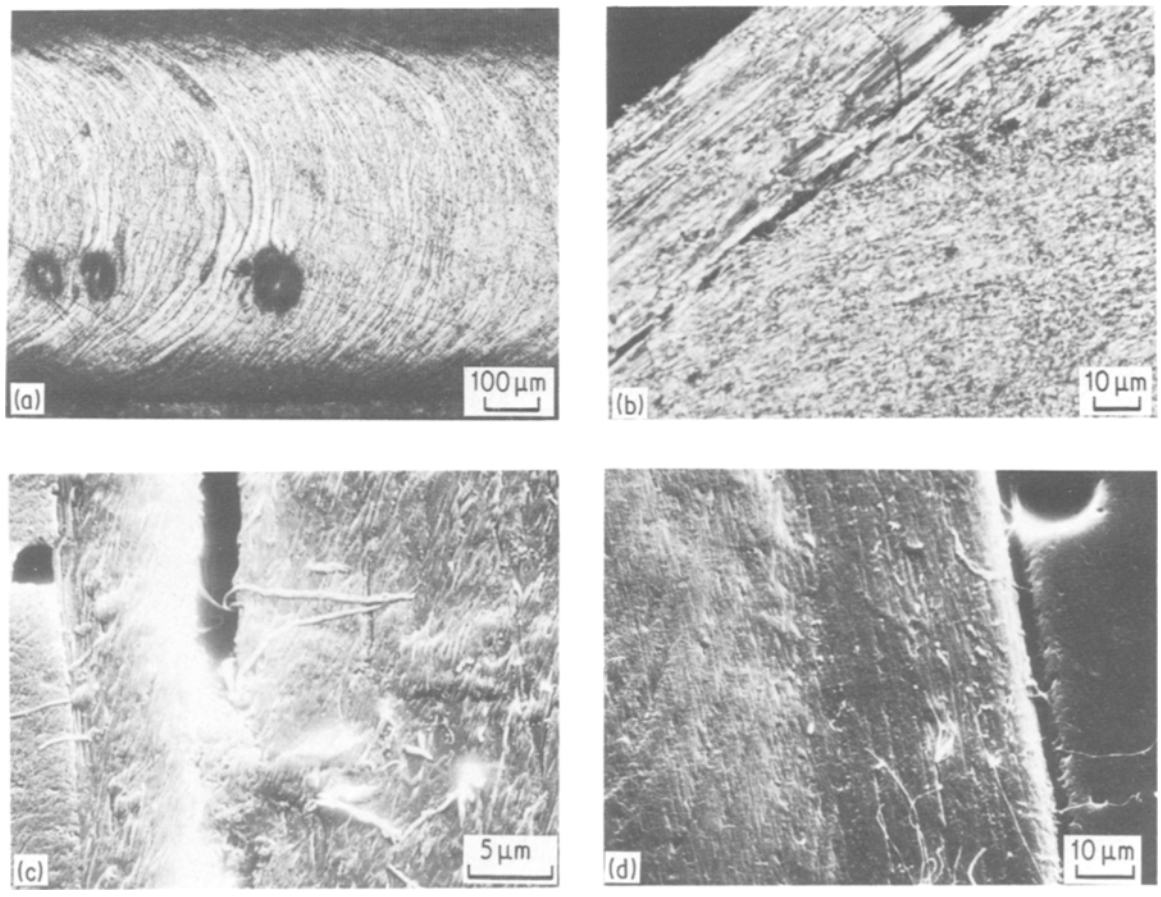

Figure 15 A polished extruded strand is shown in a reflected light micrograph (a) to have lateral flow layers and an oriented skin. A thin section, viewed in polarized light (b), reveals both a fine domain texture and an oriented skin, with an abrupt change from skin to core. Scanning electron micrographs of these polished surfaces (c and d) complement the optical study.

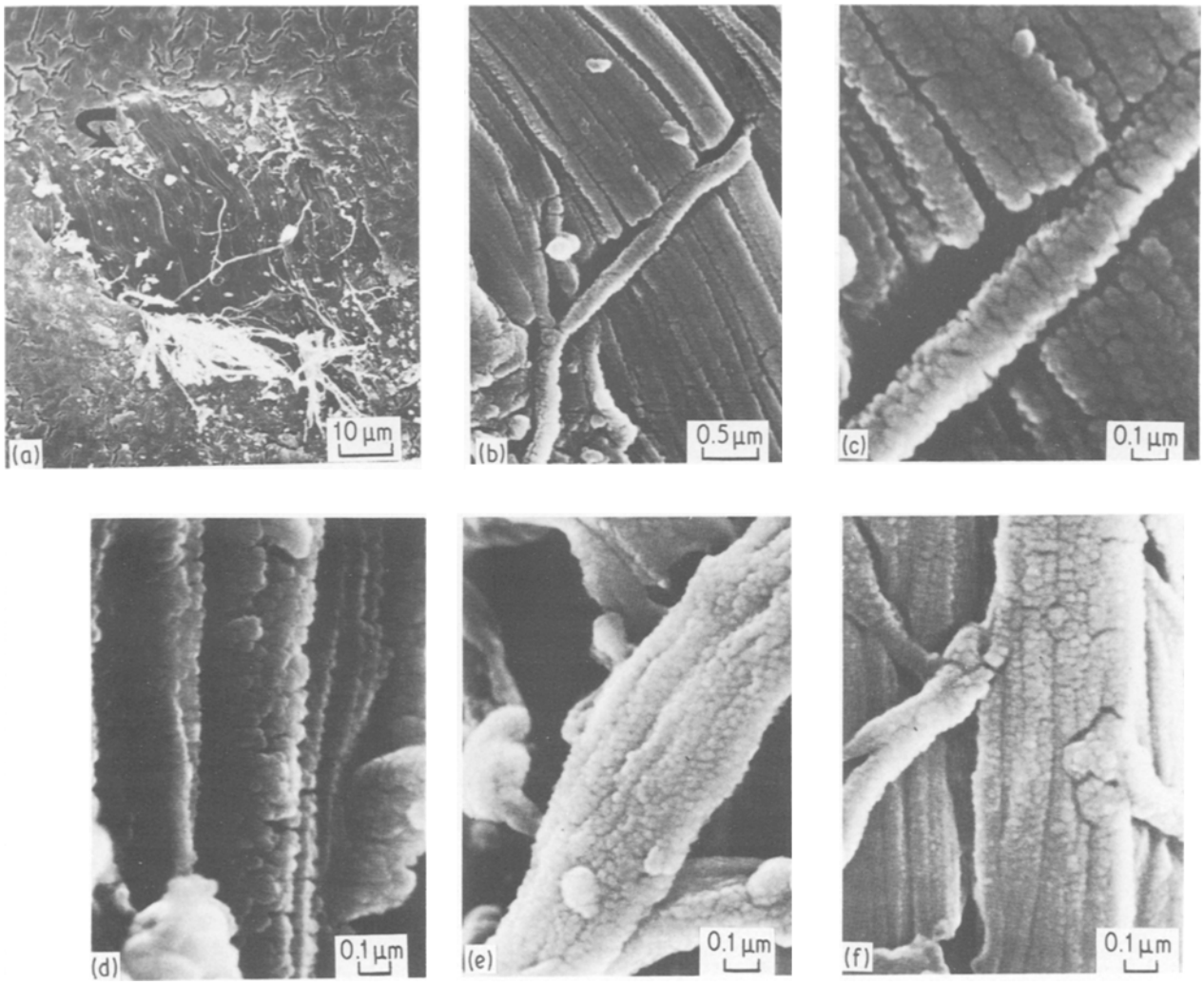

Figure 16 Plasma etching the rod shown in Fig. 15 resulted in an "uncovering" of the texture, shown in the overview SEI micrograph (a) taken about a third way into the strand. At higher magnification (b and c) the fibrillar etch texture observed is oriented in the direction of the flow lines. One fibril is seen perpendicular to the others. In an area near the outer edge of the strand, the fibrillar etch texture is oriented parallel to the strand axis (d to f).

plasma etch. Higher magnification micrographs (Figs 16b and c) reveal a fibrillar texture that is parallel to the flow lines in each region. One fibril is seen that is perpendicular to the others. In the inner skin layers the fibrillar structures are oriented parallel with the rod axis (Figs 16d to f). The fact that the etch textures observed vary in orientation, depending on location in the strand, strongly suggests that they are not a function of directionality imposed by the plasma but, rather, a function of the underlying morphology of the strand.

A micro X-ray diffraction experiment provided further information regarding the orientation in the skin and core of the moderately oriented extruded rod, shown in Figs 15 and 16. Patterns were recorded from individual 100 μm diameter areas of the skin and core. These patterns (Fig. 17) showed that the molecular axis is oriented parallel to the rod axis, with the degree of orientation varying from a high of about 13 degrees in the skin (Fig. 17a), to much lower in the core (Fig. 17b). Overall, the micrographs shown in Figs 13 to 16 are representative of the structural hierarchy typical of LCP mouldings. Variations in orientation are by complementary microscopy and X-ray diffraction experiments.

The structural textures, and their representative sizes, typical of NTP thick extrudates and moulded parts are quite uniform and they can be described by the hierarchical structural model shown in Fig. 18. The extrudate structure is shown in the artist's view, on the upper left, and in the scanning electron micrographs and optical micrographs, on the upper right, respectively. The moulded bar structure is shown in the lower drawing and scanning electron micrographs. In both cases, the sheet-like layers, observed in SEM views of the fracture surfaces, and lateral band structures seen optically, are on the order of 0.5 μm. Finer lateral striations and the fibrillar textures in the fractures, observed in the SEM, are on the order of 0.05 μm. The domain textures in all these materials are about 1 to 5 μm across, depending on the orientation. These macrostructures, at 5 μm are composed of smaller units, at two orders of magnitude smaller size. This is clearly seen in the "grains", or domains, uncovered in the etched strands, which were shown to be composed of microfibrils. Note that the characteristic layer thicknesses are consistent with the fibrillar structures representative of the fibre structure and shown in the fibre model in Fig. 8. The macrostructures and skin core textures observed in extrudates and mouldings

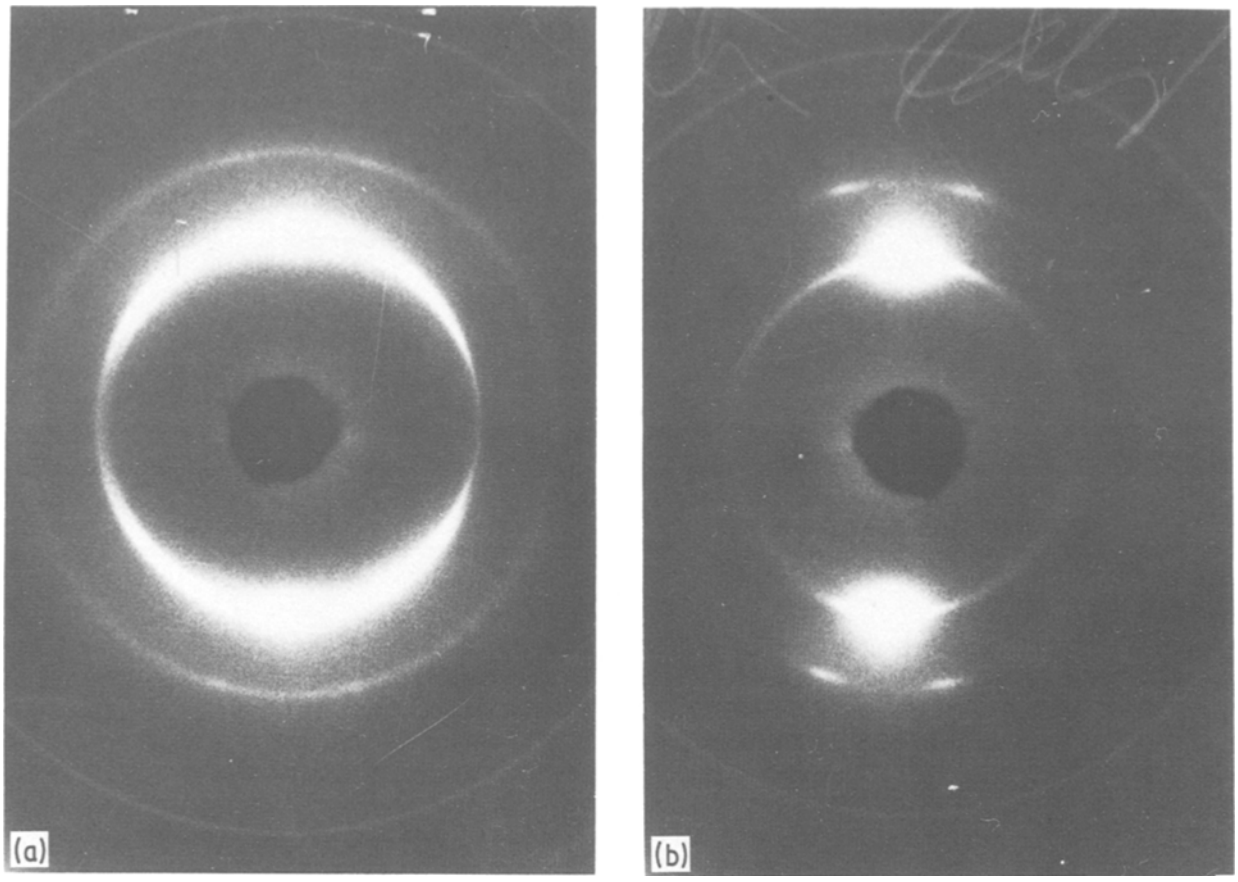

Figure 17 Micro X-ray diffraction patterns are shown recorded from 100 μm diameter areas in the skin (a) and the core (b). Note that due to the polishing method used a small portion of the opposite side of the strand was sampled by the X-ray experiment of the core region, resulting in some evidence of orientation which is due to the skin.

differ only in degree and, most importantly, the basic building blocks of all the fabricated forms investigated appear to be the same.

4. Discussion

A comparison of the observed morphology of LCP fibres, thick extrudates and injection mouldings reveals a consistent microstructure composed of fibrallar units organized in a hierarchical structure, as illustrated in Fig. 8. Although the evidence is less clear, it appears that a "defect hierarchy", a periodic spacing of defects through the microstructure, is also quite representative of LCP structures in the solid state. It is evident, however, that the details of how the hierarchical units are arranged within a given specimen is a strong function of the process and polymer history of that sample.

From the evidence presented here, not much can be said about the length of the fibrillar units other than to observe that fibrillar ends are rarely, if ever, seen. Laterally, the fibrils are identified by a characteristic minimum dimension which defines the hierarchy, and a larger, more variable lateral dimension which is related to process history. It is universally observed that highly oriented polymers possess a microfibrillar morphology: for details see the chapter, "Comparisons between Synthetic and Natural Microfiber Systems", by Sawyer and George [76], the recent books by Ciferri and Ward [2], and Zachariades and Porter [3]. Major unanswered questions are:

1. What parameters control fibrillar dimensions?
2. Are thinner fibrils caused by fractures of larger fibrils, i.e. are the structural observations *a priori* or *a posteriori* events?

The evidence presented here suggests the fibrillar structures exist prior to sample preparation for microscopy. The similarity of fibrillar minimum lateral sizes observed over a broad range of LCP samples suggest that a minimum stable size exists for microfibrillar structures. The larger, lateral dimension of the fibrillar structures seem to be a consequence of the geometry and gradients of the stress and temperature fields during formation. For example, the "fibrils" are fibre-like in fibre samples, tape-like in thick extrudates and sheet-like in injection-moulded bars. Periodic defect structures are commonly observed in highly oriented systems. Etch patterns very similar to those observed with the NTPs have been published for PPTA [23, 70] and the persistence of long periods in ultra-drawn polyethylene has been noted (see for example Ciferri and Ward [2] and others [3], etc.). In polyethylene, the origin of the long period is not attributed to the persistence of the original lamellar structure from which the highly oriented structure is drawn, but rather to the thermal history of the newly drawn material [55, 56]. Interestingly, the models advanced to explain conventional polymer drawing, such as the elegant treatment by Peterlin [53–56], define a fibrillar hierarchy in the final state which is caused by the organization of the precursor material prior to drawing.

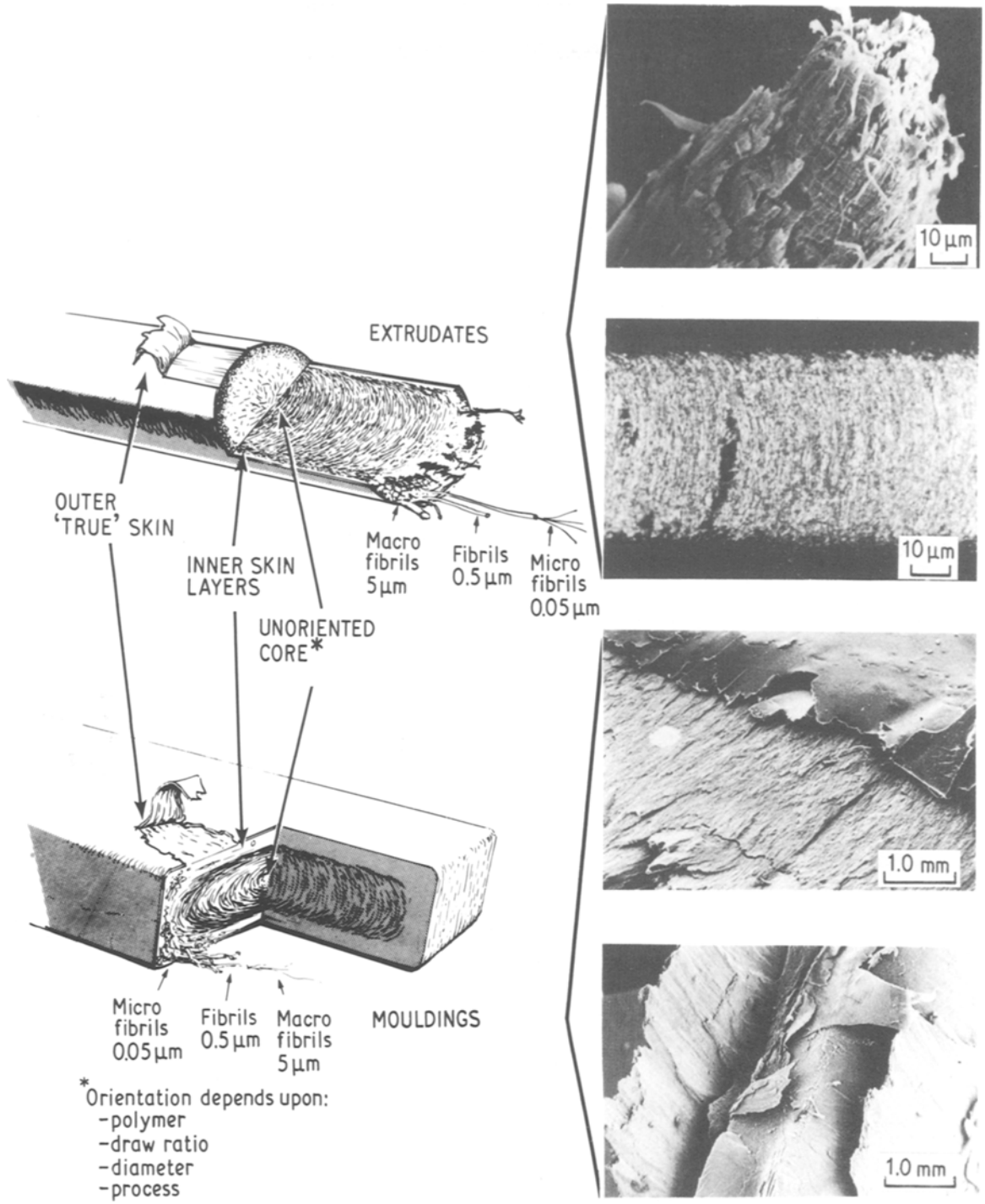

Figure 18 The LCP polymer structures of extrudates (top) and mouldings (bottom) are shown in both the artists views (left) and by micrographs (right).

Also implicit in these models, and experimentally verified, is that the diameter of the microfibrils will vary with draw ratio [7]. While it is beyond the scope of this work to address these points in detail, if one hypothesizes that the "domain" structure of the LCP mesophase is analogous to the spherulitic starting state of highly drawn conventional polymers, a unified concept of highly oriented polymer structure formation could result.

The key to the understanding of the structure–property relationships of LCPs, and other highly oriented polymer systems, is the mechanism of stress transfer between structural units. It has been shown in detail by Ciferri and Ward [2] that the mechanical properties of highly oriented polymers follow composite mechanics concepts (aggregate model [74, 75]). In high-modulus polyethylene taut tie molecules in parallel with the oriented crystal structure (intrafibrillar ties), coupled with many chains traversing several crystalline regions (interfibrillar ties), is the accepted stress transfer model [2, 55, 56]. Similarly, duPont scientists explain the high mechanical properties of PPTA in spite of an axially periodic defect layer, within the fibrillar structure, in terms of chains achieving crystallographic registry in several crystalline regions in axial proximity, i.e. the persistence length of the molecular chain is greater than the average axial distance between the crystallites. The similarity of

NTP behaviour to PPTA, in this regard, implies mechanistic equivalence; it is evident that the true, three-dimensional crystallographic registry of PPTA is not necessary for this stress transfer to efficiently occur. The solid state order of the NTPs is less than fully three-dimensional, as described by Stamatoff [29] and Blackwell [66]. For the stiff chain polymers, the important question of interfibrillar stress transfer has not been fully resolved. Possible mechanisms include:

1. Interfibrillar tie molecules, in analogy to polyethylene;
2. Interfibrillar "tie fibril", as hypothesized by Weng *et al.* for NTP mouldings [71];
3. A fibrillar network, as hypothesized by Allen *et al.* in PBT [20];
4. Interfibrillar friction due to the tortuosity and proximity of fibrillar units;
5. Interchain interactions – strong evidence points to chain slippage as the ultimate failure mechanism of LCPs (see the work of Yoon [33]).

It has been shown that as the process history of an NTP becomes more complex, the sample microstructure also becomes more complex, as evidenced by macro-layers, orientational variations, skin core effects, etc. To a large extent, the observed solid state complexity is a reflection of the ease with which NTP molecules will orient in an elongational flow field [30, 31, 41]. The often observed skin core structure is a consequence of the very high mechanical anisotropy of NTPs; as the outer layer of a specimen is aligned its modulus increases dramatically. This leads to a non-uniform stress distribution across the specimen with the proportion of the forming stress supported by the high modulus "skin" increasing. This causes an effective lowering of the stress on the sample interior; hence, a lower orientation in the core. As the orienting field is increased this "orientation front" will proceed through the sample. The apparent sharpness of the skin core boundary is also a consequence of the very high mechanical anisotropy of the LCP molecules. The very complex orientational variations observed in LCP mouldings is a consequence of the complexities of mould filling flows, as discussed by Ide and Ophir [30, 31], Garg and Kenig [32], Thapar and Bevis [41] and Weng *et al.* [71]. Once the orientational distribution in the layers is elucidated, mechanical properties may be understood in terms of composite theory [2, 74, 75].

5. Conclusions

It has been shown that the microstructure of a broad range of LCP specimens, including fibres, thick extrudates and injection-moulded parts, may be described by a hierarchial model which is composed of similar fibrillar subunits, as shown in Fig. 8. The layering, orientational variations and skin core effects, observed in thick samples produced in complex flow fields, are shown in the model in Fig. 18. These structures are a consequence of the response of the basic hierarchical units to the formation environment. Superimposed on the structural hierarchy there appears to be a defect hierarchy, as manifested by both a banded texture (500 nm and 50 nm) and regular etch patterns (50 nm). These conclusions are consistent with structural information published on other high modulus polymer systems, such as PPTA [23, 43], ordered polymers [18, 20], and ultra-oriented polyethylene [2, 3, 56]. It is suggested that the basic structure of all highly oriented polymer systems might be described by a single structural model.

Acknowledgements

The authors gratefully acknowledge the contributions of the many members of the Celanese technical staff whose skill, discussions and insights made this compilation possible. Special thanks are due to Drs Ian Hay, Kurt Wissbrun, Hyun Yoon, Jim Stamatoff, Gerry Farrow and Sunil Garg for their dedicated efforts toward the understanding of LCP structure. Special thanks are also due Mrs Madge Jamieson and Mr Roman Brozynski for their superb microscopy. The hierarchical thoughts of our CWRU colleagues in CAPRI, E. Baer, A. Hiltner and T. Weng are recognized and appreciated.

References

1. G. CALUNDANN and M. JAFFE, in Proceedings of The Robert A. Welch Conferences on Chemical Research XXVI. Synthetic Polymers, Houston, Texas, 15 to 17 November, 1982 (R. A. Welch Foundation, Houston, 1983) p. 247.
2. A. CIFERRI and I. M. WARD (Eds), "Ultra-high Modulus Polymers" (Applied Science, London, 1979).
3. A. ZACHARIADES and R. S. PORTER (Eds), "The Strength and Stiffness of Polymers" (Marcel Dekker, New York, 1983).
4. B. KALB and A. J. PENNINGS, *J. Mater. Sci.* **15** (1980) 2584.
5. J. SMOOK, M. FLINTEMAN and A. J. PENNINGS, *Polym. Bull.* **2** (1980) 775.
6. *Idem, J. Mater. Sci.* **19** (1984) 31.
7. G. CAPACCIO, A. G. GIBSON and I. M. WARD, in "Ultra-high Modulus Polymers", edited by A. Ciferri and I. M. Ward (Applied Science, London, 1979) p. 1.
8. A. E. ZACHARIADES, W. T. MEAD and R. S. PORTER, *ibid.*, p. 77.
9. G. CAPACCIO and I. M. WARD, *Nature* **243** (1973) 130, 143.
10. *Idem, Polymer* **15** (1974) 233.
11. G. CAPACCIO, A. CROMPTON and I. M. WARD, *J. Polym. Sci. Phys. Ed.* **14** (1976) 1641.
12. E. S. CLARK and L. S. SCOTT, *Polym. Eng. Sci.* **14** (1974) 682.
13. D. L. CANSFIELD, G. CAPACCIO and I. M. WARD, *Polym. Eng. Sci.* **16** (1976) 721.
14. A. CIFERRI and B. VALENTI, in "Ultra-high Modulus Polymers", edited by A. Ciferri and I. M. Ward (Applied Science, London, 1979) p. 1.
15. A. CIFERRI, W. R. KRIGBAUM and R. B. MEYER (Eds), "Polymer Liquid Crystals" (Academic, New York, 1982).
16. M. G. DOBB and J. E. McINTYRE, Properties and Applications of Liquid-Crystalline Main-Chain Polymers, in "Advances in Polymer Science 60/61" (Springer-Verlag, Berlin, 1984).
17. S. L. KWOLEK, US Pat. no. 3 600 350 (1971).
18. E. J. ROCHE, T. TAKAHASHI and E. L. THOMAS, in "Fiber Diffraction Methods", edited by A. D. French and K. H. Gardner A.C.S. Symposia Series No. 141 (A.C.S., Washington DC, 1980) p. 303.
19. E. J. ROCHE, R. S. STEIN and E. L. THOMAS, *J. Polym. Sci. Polym. Phys. Ed.* **18** (1980) 1145.
20. S. R. ALLEN, A. G. FILLIPPOV, R. J. FARRIS and E. L. THOMAS, in "The Strength and Stiffness of Polymers", edited by A. Zachariades and R. S. Porter (Marcel

Dekker, New York, 1984) p. 357.
21. W. J. JACKSON Jr and H. F. KUHFUSS, *J. Polym. Sci. Polym. Chem. Ed.* **14** (1976) 2043.
22. W. C. WOOTEN Jr, F. E. McFARLANE, T. F. GRAY Jr and W. J. JACKSON Jr, in "Ultra-high Modulus Polymers", edited by A. Ciferri and I. M. Ward (Applied Science, London, 1979) p. 227.
23. M. PANAR, P. AVAKIAN, R. C. BLUME, K. H. GARDNER, T. D. GIERKE and H. H. YANG, *J. Polym. Sci. Polym. Phys. Ed.* **21** (1983) 1955.
24. M. G. NORTHOLT, *Polymer* **21** (1980) 1199.
25. J. R. SCHAEFGEN, T. I. BAIR, J. W. BALLOU, S. L. KWOLEK, P. W. MORGAN, M. PANAR and J. ZIMMERMAN, in "Ultra-high Modulus Polymers", edited by A. Ciferri and I. M. Ward (Applied Science, London, 1979) p. 173.
26. R. N. DeMARTINO, *J. Appl. Polym. Sci.* **28** (1983) 1805.
27. M. JAFFE, *A.C.S. Div. Polym. Chem. Polym. Preprints* **19** (1978) 355.
28. L. C. SAWYER, *J. Polym. Sci. Polym. Lett. Ed.* **22** (1984) 347.
29. J. B. STAMATOFF, *Mol. Cryst. Liq. Cryst.* **110** (1984) 75.
30. Y. IDE and Z. OPHIR, *Polym. Eng. Sci.* **23** (1983) 261.
31. Z. OPHIR and Y. IDE, *ibid.* **23** (1983) 792.
32. S. GARG and S. KENIG, to be published.
33. H. Y. YOON, to be published.
34. P. J. FLORY, *Proc. Roy. Soc.* **A234** (1956) 73.
35. *Idem*, Molecular Theories of Liquid Crystals, in "Polymer Liquid Crystals", edited by A. Ciferri, W. R. Krigbaum and R. B. Meyer (Academic, New York, 1982) Ch. 4.
36. K. F. WISSBRUN, *Brit. Polym. J.* (1980) 163.
37. *Idem, J. Rheology* **25** (1981) 619.
38. K. F. WISSBRUN and A. C. GRIFFEN, *J. Polym. Sci. Polym. Phys. Ed.* **20** (1982) 1835.
39. C. P. WONG, H. OHNUMA and G. C. BERRY, *J. Polym. Sci. Polym. Symp.* **65** (1978) 173.
40. Z. TADMOR and C. G. GOGOS, "Principles of Polymer Processing" (Interscience, New York, 1979).
41. H. THAPAR and M. BEVIS, *J. Mater. Sci. Lett.* **2** (1983) 733.
42. B. WUNDERLICH and J. GREBOWICZ, *Adv. Polym. Sci.* **60** (1984) 1.
43. M. G. DOBB, D. J. JOHNSON and B. P. SAVILLE, *J. Polym. Sci.* **15** (1977) 2201.
44. M. G. DOBB, A. M. HENDELEH, D. J. JOHNSON and B. P. SAVILLE, *Nature* **253** (1975) 189.
45. S. C. BENNETT, M. G. DOBB, D. J. JOHNSON, R. MURRAY and B. P. SAVILLE, in Proceedings EMAG 75, Bristol, (Academic, London, 1976) p. 329.
46. M. G. DOBB, D. J. JOHNSON and B. P. SAVILLE, *J. Polym. Sci. Polym. Symp.* **58** (1977) 237.
47. R. HAGEGE, M. JARRIN and M. J. SOTTON, *J. Microsc.* **115** (1979) 65.
48. D. J. BLUNDELL, *Polymer* **23** (1982) 359.
49. C. VINEY, A. M. DONALD and A. H. WINDLE, *J. Mater. Sci.* **18** (1983) 1136.
50. A. M. DONALD and A. H. WINDLE, *J. Mater. Sci.* **18** (1983) 1143.
51. A. M. DONALD, *Phil. Mag.* **A47** (1983) L13.
52. J. R. SCHAEFGEN, in "The Strength and Stiffness of Polymers", edited by A. Zachariades and R. S. Porter (Marcel Dekker, New York, 1984) p. 327.
53. A. PETERLIN, *J. Mater. Sci.* **6** (1971) 490.
54. *Idem, Polym. Eng. Sci.* **18** (1978) 277.
55. *Idem*, in "Ultra-high Modulus Polymers", edited by A. Ciferri and I. M. Ward (Applied Science, London, 1979) p. 279.
56. *Idem*, in "The Strength and Stiffness of Polymers", edited by A. Zachariades and R. S. Porter (Marcel Dekker, New York, 1984) p. 97.
57. J. I. GOLDSTEIN, H. YAKOWITZ, D. E. NEWBURY, E. LIFSHIN, J. W. COLBY and J. R. COLEMAN, "Practical SEM" (Plenum, New York, 1975).
58. R. G. SCOTT, "Symposium on Microscopy", ASTM Special Publication no. 257 (1959) 121.
59. E. S. SHERMAN and E. L. THOMAS, *J. Mater. Sci.* **14** (1979) 1109.
60. L. C. SAWYER, in Proceedings of the 39th Annual Meeting of the EMSA, edited by G. W. Bailey (Claitors, Baton Rouge, 1981) p. 334.
61. T. SARADA, L. C. SAWYER and M. OSTLER, *J. Memb. Sci.* **15** (1983) 97.
62. P. G. de GENNES, "The Physics of Liquid Crystals" (Oxford University Press, 1979).
63. D. DEMUS and L. RICHTER, "Textures of Liquid Crystals" (Verlag Chemie, New York, 1978).
64. S. C. SIMMENS and J. W. S. HEARLE, *J. Polym. Sci. Polym. Phys. Ed.* **18** (1980) 871.
65. M. G. DOBB, D. J. JOHNSON and B. P. SAVILLE, *Polymer* **22** (1981) 961.
66. G. A. GUTIERREZ, R. A. CHIVERS, J. BLACKWELL, J. B. STAMATOFF and H. N. YOON, *ibid.* **24** (1983) 937.
67. J. R. MINTER, K. SHIMAMURA and E. L. THOMAS, *J. Mater. Sci.* **16** (1981) 3303.
68. A. D. G. STEWART and M. W. THOMPSON, *ibid.* **4** (1969) 56.
69. S. B. WARNER, D. R. UHLMANN and L. H. PEEBLES, *ibid.* **10** (1975) 758.
70. L. S. LI, L. F. ALLARD and W. C. BIGELOW, *J. Macromol. Sci. Phys.* **B22** (1983) 269.
71. T. WENG, A. HILTNER and E. BAER, *J. Mater. Sci.*
72. M. R. KANTZ, H. D. NEWMAN and F. H. STIGALE, *J. Appl. Polym. Sci.* **16** (1972) 1249.
73. S. Y. HOBBS and C. F. PRATT, *ibid.* **19** (1975) 1701.
74. P. J. BARHAM and R. G. C. ARRIDGE, *J. Polym. Sci. Polym. Phys. Ed.* **15** (1977) 1177.
75. R. G. C. ARRIDGE and P. J. BARHAM, *Polymer* **19** (1978) 654.
76. L. H. SAWYER and W. GEORGE, in "Cellulose and Other Natural Polymer Systems: Biogenesis, Structure, and Degradation", edited by R. Malcolm Brown Jr (Plenum, New York, 1982) p. 429.

Received 11 April
and accepted 11 July 1985